*Indian J Phys (February 2015) 89(2):107–114*
DOI 10.1007/s12648-014-0559-6

ORIGINAL PAPER

# A study on optimum transition state and tautomeric structures of a bis-heterocyclic monoazo dye

**M Karakaya[1]* and M Yildiz[2]**

[1]Department of Energy Systems, Engineering and Architecture Faculty, Sinop University, 57000 Sinop, Turkey

[2]Department of Physics, Faculty of Sciences, Karamanoglu Mehmetbey University, 70100 Karaman, Turkey

Received: 26 January 2014 / Accepted: 16 July 2014 / Published online: 13 August 2014

**Abstract:** In this study, possible tautomeric forms and ground state conformers of a bis-heterocyclic monoazo dye, 4-[ethyl 4′-methyl-5′-(phenylcarbamoyl)thiophene-3′-carboxylate-2′-ylazo]-3-methyl-1H-pyrazolin-5-one, have been calculated using density functional theory methods with 6-31G (*d*) basis set. $^{1}H$ and $^{13}C$ chemical shifts of tautomeric forms have been calculated. Calculated vibrational frequencies and chemical shifts have been compared with corresponding experimental data. Using time-dependent Hartree–Fock method, electronic absorption spectrum of title compound has been calculated and compared with experimental maximum wavelength data. Quantum Synchronous Transit2 approaches have been used for finding the optimum transition state and tautomeric forms of studied molecule. Calculations have shown that the most probable preferential form of this molecule in ground state is hydrazo-keto form. The calculations of frontier molecular orbitals and first order hyperpolarizability have also confirmed this stability.

**Keywords:** Bis-heterocyclic monoazo dyes; Tautomeric form; Infrared spectra; Density functional theory

**PACS No.:** 31.15.−p

## 1. Introduction

Azo compounds are quite colorful and have been extensively used in many technical applications such as coloring fibers, photo electronic applications, printing systems, optical storage technology, textile dyes as well as in many biological reactions [1–10]. Azo moieties have fungicidal and antibacterial properties and are used in the detection of trace metals in drinking water and food materials [11]. Monoazo disperse dyes with heterocyclic diazo components have been applied to hydrophobic fibres in commercial area [12]. Many articles on synthesis and dyeing properties of thiophene based azo dyes for synthetic fibres and collated polyester and wool fibres, are available [13–16]. Thiophene-containing azo dyes, on the other hand, have many advantages including a color deepening effect, as the molecular structure provides better dye ability. Heterocyclic nature of thiophene ring has also provided an opportunity for perfect sublimation fastness on the dyed fibers [17–19]. In conjunction to such compounds, synthesis and spectral properties of some heterocyclic azo dyes have been reported [20–22]. Also, absorption abilities and tautomeric structures of some bis-heterocyclic monoazo dyes based on thiophene ring have been examined by some researchers [23].

Purpose of this study is to investigate a bis-heterocyclic monoazo dye, 4-[ethyl 4′-methyl-5′-(phenylcarbamoyl)thiophene-3′-carboxylate-2′-ylazo]-3-methyl-1H-pyrazolin-5-one theoretically, based on thiophene ring. In present study, optimized molecular geometries for tautomeric forms of this monoazo dye have been computed in order to establish the most stable ground state configuration. Thereafter, vibrational frequencies, $^{1}H$ and $^{13}C$ nuclear magnetic resonance (NMR) shift values of their designed most stable conformers have been calculated. Combined studies of NMR and electronic spectroscopies have been recently carried out on various molecular systems by quantum chemistry calculation methods [24–26].

## 2. Calculation methods

Vibrational frequencies and optimized structures for three tautomeric forms of studied molecule were calculated by using ab initio density functional theory (DFT/B3LYP

*Corresponding author, E-mail: mkarakayafizik@hotmail.com

functional) methods at 6-31G (*d*) basis set level. All computations were performed using Gaussian 09 program package [27] and Gauss-View molecular visualization program [28] on personal computer. For computed frequencies, the scale factor of 0.9613 was used for B3LYP [29]. Vibrational assignments with the help of normal coordinate analysis (NCA) were made on the basis of potential energy distribution (PED) calculated by using Vibrational Energy Distribution Analysis (VEDA 4) program [30, 31]. In chemical shift calculations tetramethylsilane (TMS) was used as a reference molecule, and theoretical chemical shift $^{1}$H and $^{13}$C values were obtained by subtracting gauge-including atomic orbital (GIAO) isotropic magnetic shielding (IMS) values using DFT method at 6-31G (*d*) basis set level [32, 33]. Electronic absorption spectra were also calculated using time-dependent unrestricted HF (TD-UHF) method at 6-31G (*d*) basis set level. For locating transition structures the *Synchronous Transit-Guided Quasi-Newton* (STQN) Method, developed by Schlegel and coworkers [34, 35], used a linear synchronous transit to get closer to the quadratic region around the transition state and then used a quasi-Newton or eigenvector-following algorithm to perform the optimization. To find optimum transition states of these compounds, Quantum Synchronous Transit2 (QST2) approaches were used by taking their optimized tautomeric forms for azobenzene derivatives in previous study [36, 37].

## 3. Results and discussion

### 3.1. Potential energy surface scans and conformation analysis

In order to find the most stable conformers of studied compound and its tautomeric forms, detailed potential energy surface (PES) scans for $\tau_1$, $\tau_2$ and $\tau_3$ torsion angles have been performed. These essential torsion angles used for PES scans on azo-enol form are given in Fig. 1. For azo-enol form,

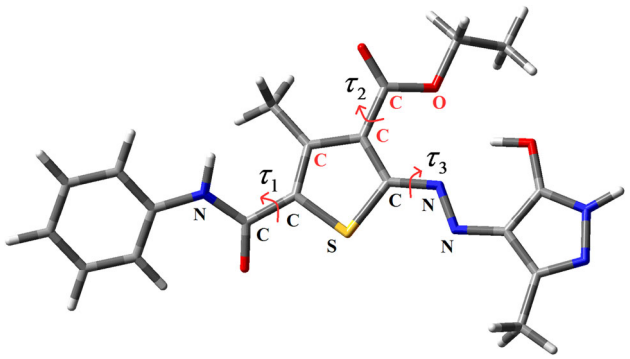


**Fig. 1** Essential torsion angles on azo-enol form of studied compound for potential energy surface scans

scans are performed by changing $\tau_1$ dihedral angle every 30° for 360° rotation (from 0° to 360°) and and $\tau_2$ dihedral angle every 30° for 360° rotation (from 180° to 540°) around the bond in steps 144, simultaneously. Then, scans have been performed by changing $\tau_3$ dihedral angle every 10° from −180° to 180° for obtained minimum energy structures. All of PES scans have been performed by semi-empirical/Restricted Austin Model 1 (RAM1) method due to high number of scan steps and faster calculations in large molecules. Scan results on $\tau_1$ and $\tau_2$ dihedral angles for azo-enol structure are given in Fig. 2(a). Graph obtained by change of the$\tau_3$ dihedral angle is also shown in Fig. 2(b). After scanning, three low-energy conformers have been optimized by DFT (B3LYP) method at 6-31G (*d*) basis set.

$\tau_1$, $\tau_2$ and $\tau_3$ dihedral angles calculated by using DFT/B3LYP method at 6-31G (*d*) basis set level for all the conformers of azo-enol form are listed in Table 1. Also, electronic energies, relative energies and mean vibrational deviations are given in Table 1. Relative energy values and calculated vibrational deviations, point to the lowest energy conformer I. As seen Table 1, mean vibrational deviation increases while relative energy increases. Relative energies and mean calculated vibrational deviations between conformers I and II or I and III are fairly high. Similar theoretical approach and analysis have been introduced to determine the low-energy structures for halogen-substituted acetylcholine compounds in previous study [38].

### 3.2. Optimized structures of tautomeric forms

Minimum energy optimized molecular structure and tautomeric forms (azo-enol and hydrazo-keto form) of studied compound with numeration of atoms are shown in Fig. 3(a)–3(c), respectively. All of these structures are obtained by using DFT/B3LYP method at 6-31G (*d*) basis set. Then, PES scans have been done by changing of bond length tautomeric O–H from 0.90 to 2.00 Å in steps of 0.05 Å using DFT–B3LYP methods at 6-31G (*d*) basis set. These results are shown in Fig. 4. As seen from the Fig. 4, hydrazo-keto form of the molecule is more stable. Relative and barrier energy values between the azo-enol and hydrazo-keto forms are 9.7, 12.9 kcal/mol, respectively.

### 3.3. Vibrational analysis

To find out the optimized geometry of studied compound, all selected computed frequencies and proposed vibrational assignments together with IR intensity are listed in Table 2. Experimental stretching vibration values are also given in this table [23]. Assignments of selected vibrational modes obtained by using VEDA 4 program are also given in Table 2. For calculated frequencies, values at DFT method are as follows: 3,521 and 3,485 $cm^{-1}$ for NH, 3,089 $cm^{-1}$

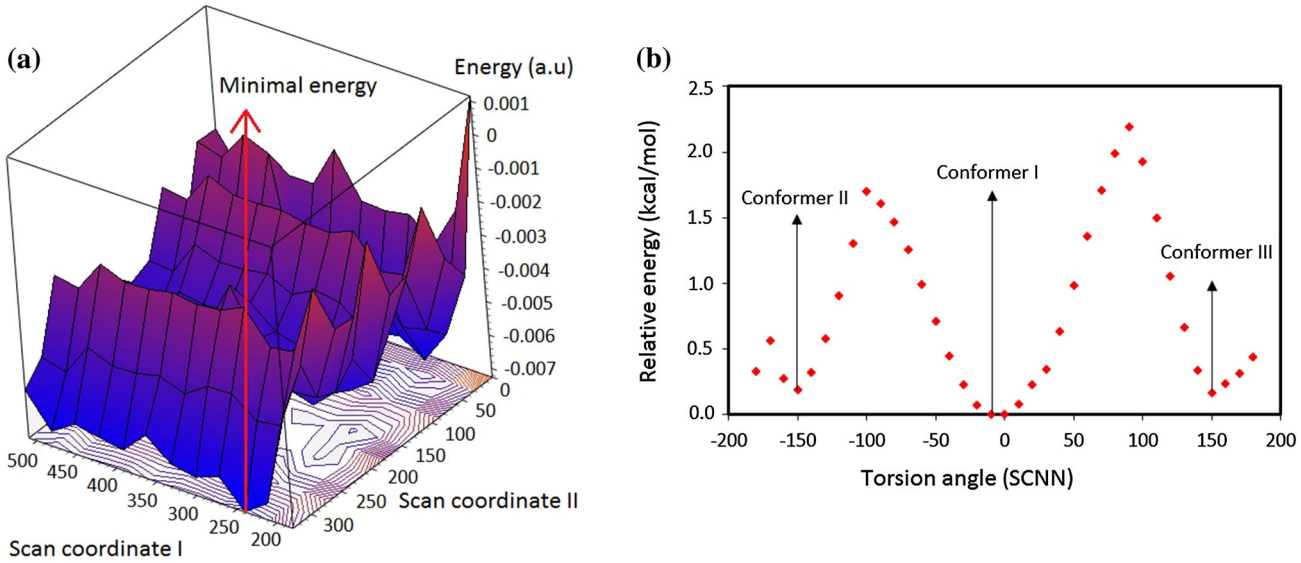


**Fig. 2** Potential energy surface scan of azo-enol form of studied compound for selected torsional angles. (**a**) $\tau_1$[NCCS], $\tau_2$[CCCO] (simultaneously) and (**b**) $\tau_3$[SCNN]

**Table 1** Sum of electronic and zero point energies, relative energies and mean calculated vibrational deviations between conformers of azo-enol form at density functional theory, 6-31G (*d*) basis set

| Conformers | $\tau_1$ | $\tau_2$ | $\tau_3$ | Energy (Hartree/part.) | Relative energy (kcal/mol) | Vib. deviation $\lvert\Delta\nu\rvert_{ave}$ |
|---|---|---|---|---|---|---|
| *Azo-enol structure* | | | | | | |
| I | 153.6 | −155.5 | 1.2 | −1,707.916821 | 0.00 | 0.00 |
| II | 163.6 | −131.5 | −152.6 | −1,707.907028 | 6.15 | 5.68 |
| III | 169.1 | 127.5 | 154.3 | −1,707.906948 | 6.20 | 6.36 |

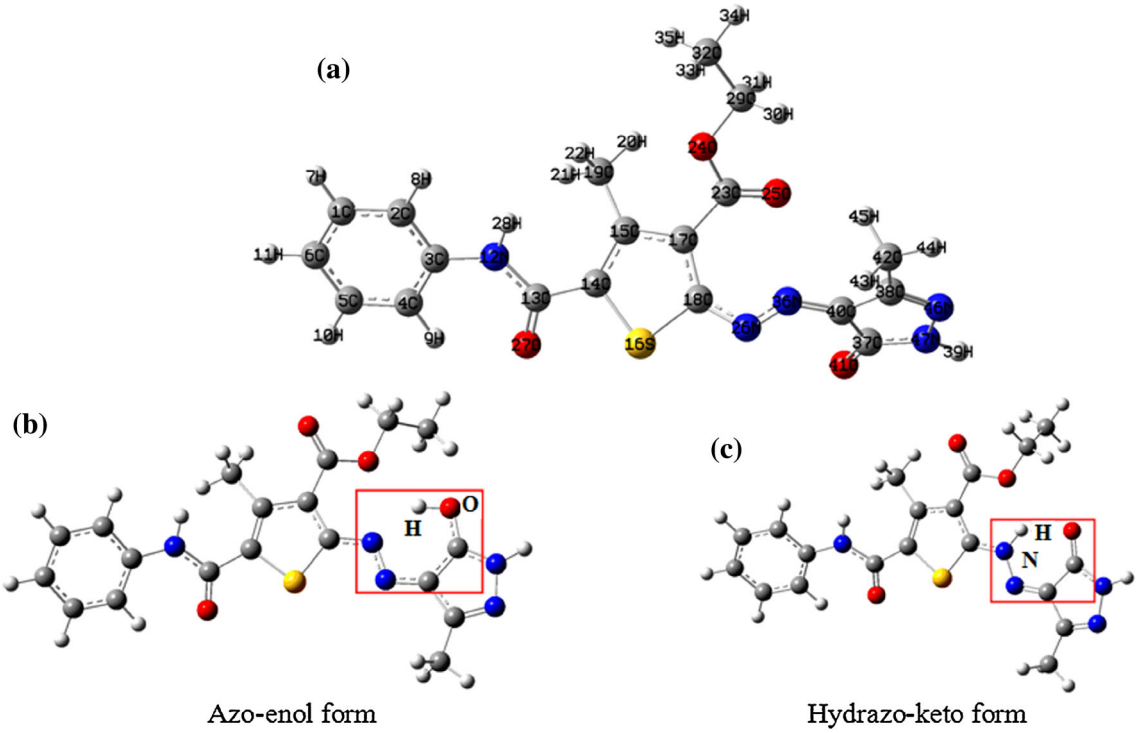


**Fig. 3** Calculated optimized structures for (**a**) studied compound, (**b**) azo-enol form and (**c**) hydrazo-keto form

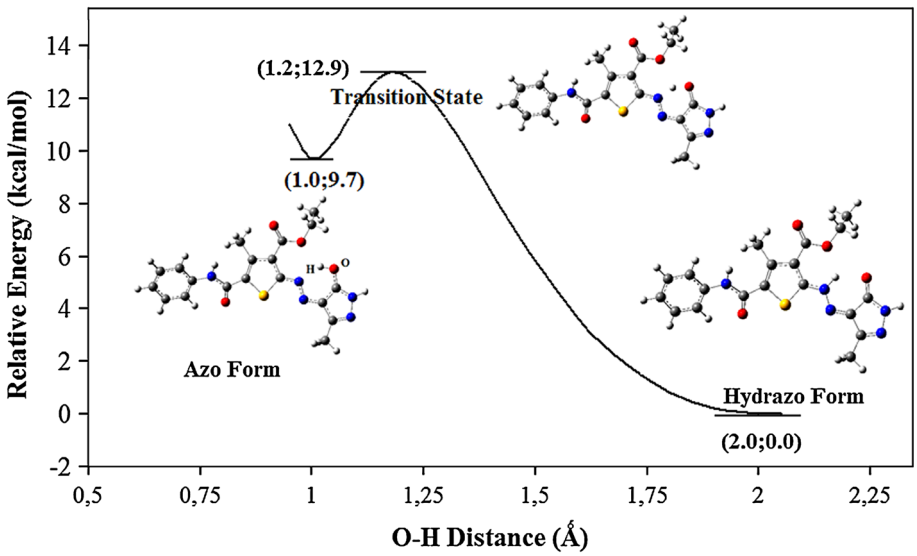


**Fig. 4** Potential energy surface scan graph for tautomeric forms of studied compound

**Table 2** Selected vibrational wavenumbers obtained for studied compound at density functional theory, 6-31G (*d*) basis set

| Experimental IR[a] Frequencies ($cm^{-1}$) | Density functional theory B3LYP functional | | Vibrational assignments and %PED[b] |
|---|---|---|---|
| | Calculated frequencies ($cm^{-1}$) (scaled) | IR intensity (km/mol) | |
| 3,259 ν(N–H) | 3,521 | 93 | ν[Pz–NH](100) |
| 3,242–3,230 ν(N–H) | 3,485 | 15 | ν[NH](100) |
| 3,034 ν(Ar–CH) | 3,089 | 36 | ν[Ar–CH](98) |
| 2,982 ν(Al–CH) | 3,013 | 23 | ν[Al–CH](98) |
| | 2,936 | 15 | ν[Me–CH](99) |
| 1,715 ν(C=O) | 1,735 | 166 | ν[Pz–O=C](81) |
| 1,673 ν(C=O) | 1,719 | 147 | ν[O=C](88) |
| 1,645 ν(C=O) | 1,674 | 168 | ν[O=C](82) |
| | 1,575 | 75 | ν[Pz–NC](69) |
| | 1,517 | 539 | δ[Ar–HNC](45) + ν[Ar–CC](13) + ν[NC](13) |
| | 1,427 | 145 | ν[Ar–CC](13) |
| | 1,312 | 202 | ν[Ar–CC](11) + δ[Ar–HCC](11) |
| | 1,201 | 459 | ν[NC](31) + δ[Pz–OCN](10) |
| | 1,167 | 277 | ν[O–C](29) + δ[Ar–HCC](10) |
| | 1,123 | 87 | ν[N=N](26) + ν[O–C](10) |
| | 1,047 | 50 | ν[Pz–NN](59) + ν[Pz–NC](12) |
| | 1,015 | 53 | ν[CC](34) +ν[OC](31) |
| | 943 | 136 | δ[Pz–NC](27) +τ[Pz–HCCC](19) + ν[Pz–CC](13) |
| | 863 | 55 | δ[OCN](21) + δ[NCC](18) |
| | 742 | 52 | τ[Ar–HCCC](54) + γ[Ar–NCCC](11) |
| | 551 | 26 | ν[Pz–CC](15) + ν[Pz–NN](12) +δ[Pz–CNN](11) + τ[Ar–HNCC](10) |
| | 453 | 80 | τ[Pz–HNNC](46) + γ[OCOC](11) |
| | 426 | 60 | δ[Pz–OCN](10) + δ[OCC](10) |
| $R^2$ | 0.9918 | | |

ν: stretching, δ: bending, γ: out of plane bending, τ: torsion modes, Ar: aromatic, Me: methyl, Al: aliphatic, Pz: pyrazoline

[a] Taken from Ref. [23]

[b] Potential energy distribution (PED) of studied compound, less than 10 % are not shown

for C–H (aromatic), 3,013 $cm^{-1}$ for C–H (aliphatic), 1,735, 1,719 and 1,674 $cm^{-1}$ for C=O stretching. Also, frequency values for N=N stretching mode at DFT method are calculated as 1,123 $cm^{-1}$. For vibrational assignments and %PED, results of optimized structure calculated by DFT/6-31G (*d*) basis set have been used. C–H vibration is 3,089 $cm^{-1}$ at B3LYP/6-31G (*d*) level with the PED contribution of 98 %. Assignments, especially for high frequencies, in Table 2 are very similar to the known vibration assignments heterocyclic disazo dye derivatives [22]. Correlation values ($R^2$) between experimental and calculated frequencies have been computed as 0.9918 for DFT method. Incompatibility with experimental data for N–H stretching mode is noteworthy. Nevertheless, correlation values between calculated and experimental results in Table 2, generally, also show their agreement.

### 3.4. NMR spectral analysis

Isotropic chemical shifts are frequently used as an aid in identification of reactive organic as well as ionic species. It is recognized that accurate predictions of molecular geometries are essential for reliable calculations of magnetic properties [39]. Gauge-Independent Atomic Orbital (GIAO) $^{13}C$ and $^{1}H$ chemical shift calculations with respect to TMS have been made by using B3LYP/6-31G (*d*) level for studied compound and its tautomeric forms. Results of these calculations are tabulated in Table 3. Experimental $^{1}H$ NMR chemical shift values [23] are also given in Table 3, but $^{13}C$ NMR values cannot be found in the literature. Since the experimental chemical shift values for aromatic H atoms are given as 7.01–7.69 ppm, calculated $^{1}H$ NMR chemical shift values are compared with average of these experimental data. Oxygen atoms with more electronegative property, polarize the electron distribution in its bonds to adjacent carbon atoms and decrease electron density at the bridge for studied molecule. So, $^{13}C$ chemical shifts are computed as high values, 149.56, 156.35 and 154.83 ppm for 13C, 18C and 23C atoms, respectively. $^{13}C$ chemical shifts for aromatic carbons of studied compound are also computed at the range of 109.72–131.57 ppm. Correlation factors between experimental and theoretical chemical shifts can be seen in the last lines of $^{1}H$ NMR chemical shift values. Correlation values ($R^2$) between experimental and theoretical $^{1}H$ chemical shifts have been computed as 0.8297, 0.8229 and 0.7958 for studied compound and its azo-enol, hydrazo-keto tautomeric forms, respectively.

### 3.5. Non-linear optical properties

Polarizability and hyperpolarizability qualify the response of a system in an applied electric field and determine not

**Table 3** Experimental and calculated chemical shift values for studied compound and tautomeric forms

| Atoms | Experimental[a] (ppm) (solvent: DMSO-$d_6$) | B3LYP/6-31G (*d*) basis set | | |
|---|---|---|---|---|
| | | Studied compound (solvent: none) | Tautomeric forms | |
| | | | Azo-enol (solvent: none) | Hydrazo-keto (solvent: none) |
| 7-H[b] | | 7.141 | 7.126 | 7.119 |
| 8-H[b] | | 6.305 | 6.347 | 6.329 |
| 9-H[b] | 7.01–7.69 | 8.730 | 8.733 | 8.678 |
| 10-H[b] | | 7.302 | 7.263 | 7.255 |
| 11-H[b] | | 6.990 | 6.933 | 6.916 |
| 20-H | 2.09 | 2.372 | 2.630 | 3.245 |
| 21-H | 2.09 | 2.377 | 2.376 | 2.309 |
| 22-H | 2.09 | 2.255 | 2.447 | 2.239 |
| 28-H | 10.75 | 6.046 | 6.157 | 6.076 |
| 30-H | 4.31 | 4.121 | 4.663 | 4.893 |
| 31-H | 4.31 | 4.141 | 3.998 | 4.303 |
| 33-H | 1.34 | 1.443 | 1.267 | 1.668 |
| 34-H | 1.34 | 1.106 | 0.983 | 0.926 |
| 35-H | 1.34 | 1.399 | 1.760 | 1.337 |
| 39-H | 9.95 | 6.764 | 7.510 | 6.922 |
| 43-H | 1.89 | 2.058 | 2.453 | 2.176 |
| 44-H | 1.89 | 1.957 | 2.100 | 1.967 |
| 45-H | 1.89 | 2.102 | 2.420 | 2.156 |
| 48-H[c] | 9.69, 10.13 | | 11.107 | 12.958 |
| | $R^2$ | 0.8297 | 0.8229 | 0.7958 |
| 1-C | | 121.334 | 121.253 | 121.268 |
| 2-C | | 109.717 | 109.669 | 109.653 |
| 3-C | | 131.573 | 132.034 | 131.985 |
| 4-C | | 113.122 | 112.852 | 112.836 |
| 5-C | | 123.679 | 123.411 | 123.387 |
| 6-C | | 117.291 | 116.625 | 116.610 |
| 13-C | | 149.556 | 150.499 | 150.026 |
| 14-C | | 147.046 | 138.327 | 132.272 |
| 15-C | | 131.471 | 132.702 | 132.790 |
| 17-C | | 117.882 | 122.363 | 110.093 |
| 18-C | | 156.345 | 163.730 | 156.642 |
| 19-C | | 17.202 | 17.577 | 16.936 |
| 23-C | | 154.829 | 155.795 | 153.635 |
| 29-C | | 60.785 | 60.956 | 59.897 |
| 32-C | | 14.433 | 14.039 | 15.506 |
| 37-C | | 148.104 | 140.708 | 149.755 |
| 38-C | | 139.672 | 144.147 | 141.237 |
| 40-C | | 119.775 | 120.101 | 125.399 |
| 42-C | | 14.622 | 13.613 | 13.621 |

[a] Taken from Ref. [23]

[b] Exp. values 7.01–7.69 (5H. ArH)

[c] Tautomeric NH or OH

**Table 4** Electric dipole moment $\mu$(D), average polarizability ($\bar{\alpha}$) and first hyperpolarizability ($\beta$) for azo-enol and hydrazo-keto form of studied compound

| | $\mu_x$ | $\mu_y$ | $\mu_z$ | $\mu_{tot}$ | $\bar{\alpha}$ (Å$^3$) | $\beta_{tot} \times 10^{-30}$ (cm$^5$/esu) |
|---|---|---|---|---|---|---|
| *DFT method/6-31G (d) basis set* | | | | | | |
| Azo-enol form | −2.1166 | 3.8773 | −0.6009 | 4.4581 | 48.108 | 31.075 |
| Hydrazo-keto form | −1.0257 | 2.8113 | −0.7739 | 3.0910 | 47.361 | 54.948 |

only the strength of molecular interactions as well as the cross sections of different scattering and collision processes, but also the nonlinear optical properties (NLO) of the system [40, 41]. In order to investigate the relationships among photocurrent generation, molecular structures, polarizability and hyperpolarizability of studied compound and azo-hydrazo forms are calculated.

Non-linear optical response of an isolated molecule in an electric field $E_i$ ($\omega$) can be represented as a Taylor series expansion of the total dipole moment ($\mu_{tot}$) induced by the field:

$$\mu_{tot} = \mu_0 + \alpha_{ij}E_j + \beta_{ijk}E_jE_k + \cdots \quad (1)$$

where $\alpha$ is linear polarizability, $\mu_0$ is permanent dipole moment and $\beta_{ijk}$ are first hyperpolarizability tensor components. Average linear polarizabilities are defined as [42]:

$$\bar{\alpha} = \frac{\alpha_{xx} + \alpha_{yy} + \alpha_{zz}}{3} \quad (2)$$

First hyper polarizability tensor can be calculated with *x, y* and *z* components of $\beta$ and complete equation for calculating the magnitude of $\beta$ from Gaussian09 output is given as follows:

$$\beta_{tot} = [(\beta_{xxx} + \beta_{xyy} + \beta_{xzz})^2 + (\beta_{yyy} + \beta_{yzz} + \beta_{xxy})^2 + (\beta_{zzz} + \beta_{xxz} + \beta_{yyz})^2]^{1/2} \quad (3)$$

Since the values for average linear polarizabilities and first hyperpolarizability tensors of the output file of Gaussian09 are reported in atomic units (a.u.), calculated values are converted into electrostatic units, esu (1 a.u = $8.6393 \times 10^{-33}$ cm$^5$/esu). B3LYP/6-31G (*d*) results of electronic dipole moment $\mu_i = (i = x, y, z)$, polarizability and first hyperpolarizability for studied compound and its tautomeric forms are listed in Table 4. Calculated dipole moments are equal to 4.46 and 3.09 D for azo-enol and hydrazo-keto form, respectively. Calculated values of $\bar{\alpha}$ for azo-enol and hydrazo-keto form are 48.11 and 47.36 Å$^3$, shown in Table 4 and $\beta$ are also $31.08 \times 10^{-30}$ and $54.95 \times 10^{-30}$ (cm$^5$/esu), respectively. Biggest values of hyperpolarizability are noticed and subsequently delocalization of electron cloud is more in that direction and maximum $\beta$ value may be due to π-electron cloud movement from donor to acceptor, which makes the molecule highly polarized and intramolecular charge transfer (ICT) possible [43].

### 3.6. Frontier molecular orbitals (FMOs) and UV–vis absorption spectral analysis

Frontier molecular orbitals (FMOs) are important in determining such properties as molecular reactivity and ability of a molecule to absorb light. FMOs are also very important for optical and electric properties [44]. Highest occupied molecular orbital (HOMO) and lowest unoccupied molecular orbital (LUMO) are main orbitals taking part in the chemical reaction. HOMO energy characterizes the ability of electron giving, LUMO energy characterizes the ability of electron accepting and gap between HOMO and LUMO energies characterizes molecular chemical stability [45]. Molecular orbital surfaces, HOMO-1, HOMO, LUMO, LUMO + 1 and energy levels computed at B3LYP/6-31G (*d*) levels for studied compound are drawn in Fig. 5(a)–5(d), respectively. In this study, it can be said that HOMO are mainly localized on aromatic, thiophene, aliphatic and pyrazoline groups. LUMO are also localized on thiophene, aliphatic and pyrazoline groups. Molecular electronic spectrum is usually originated by the electron transition from HOMO to LUMO. Hyperpolarizability is also directly related to HOMO–LUMO energy gap. HOMO–LUMO band gaps are computed 3.043 and 3.011 eV at B3LYP/6-31G (*d*) level for azo-enol and hydrazo-keto form, respectively. It is obvious that there should be an inverse relationship between HOMO–LUMO gap and the first of hyperpolarizability [46]. Higher values of first hyperpolarizability can be achieved with lower HOMO–LUMO gaps [47]. Therefore, it can be expected that hydrazo-keto form have a bit lower HOMO–LUMO gap than azo-enol form. This situation can be attributed that HOMO–LUMO gap may be decreased by hydrogen-bonded interaction in molecular systems. Hydrazo-keto form with charge-assisted hydrogen bonding interaction has a little lower HOMO–LUMO band gap than that of azo-enol form.

Electronic values, such as absorption wavelengths, excitation energies and oscillator strengths are computed by time-dependent unrestricted Hartree–Fock (TD-UHF) method at 6-31G (*d*) basis set level as UV visible spectra analysis and tabulated in Table 5. Calculations of molecular orbital geometry show that visible absorption maxima of this molecule correspond to electron transition between frontier orbitals such as translation from HOMO-6 to LUMO + 1. For the similar bis-heterocyclic monoazo dye,

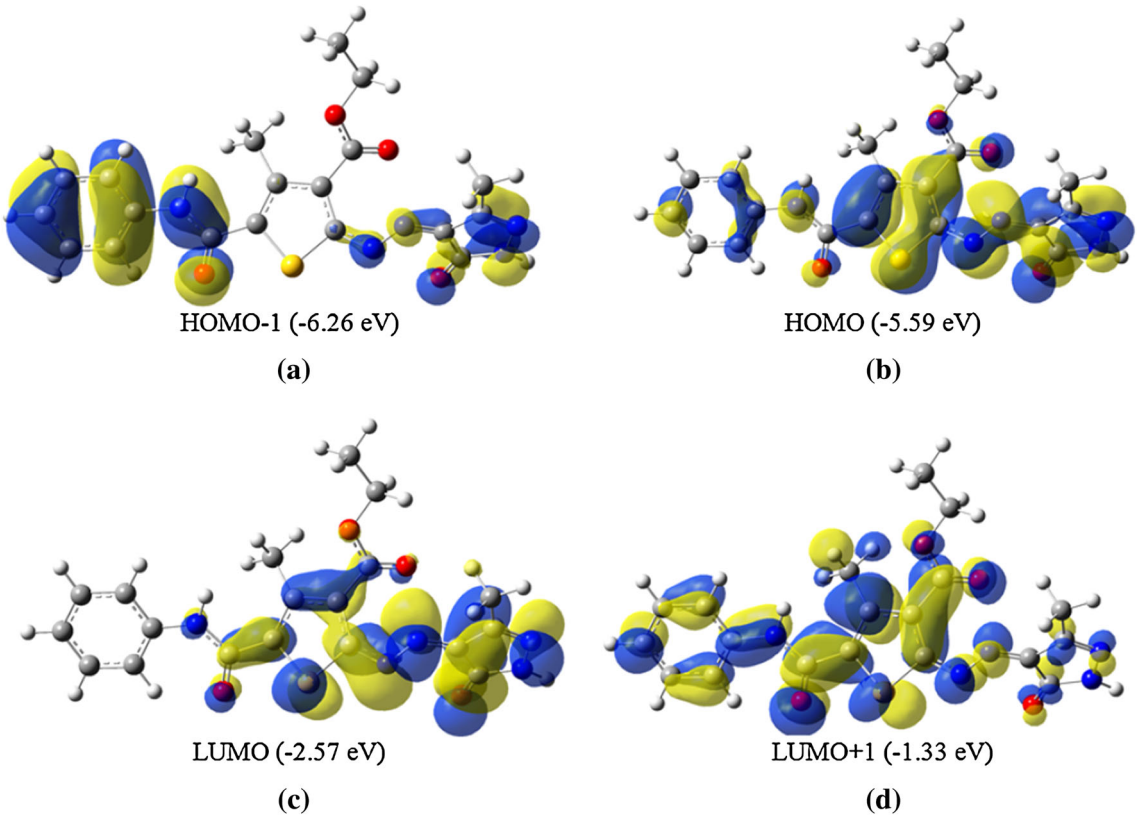


**Fig. 5** 3D plots of (**a**) HOMO-1, (**b**) HOMO, (**c**) LUMO and (**d**) LUMO + 1 distributions at B3LYP/6-31G (*d*) level of studied compound

**Table 5** Calculated wavelengths, excitation energies, oscillator strengths values for studied compound

| Wavelengths λ (nm) | Excitation energies (eV) | Assignments | Oscillator strengths (*f*) | Experimental[a] $\lambda_{max}$ (nm) | |
|---|---|---|---|---|---|
| | | | | Methanol | Chloroform |
| 432.18 | 2.8688 | H-6 → L + 1<br>H-5 → L<br>H-9 → L + 1<br>H-5 → L + 1<br>H-10 → L | 0.0021 | 467 | 452 |
| 396.79 | 3.1247 | H-6 → L + 1<br>H-6 → L<br>H-5 → L<br>H-9 → L + 1<br>H-9 → L<br>H-15 → L + 8 | 0.0012 | | |

[a] Taken from Ref. [23]

absorption maxima are observed at 445, 438 and 440 nm by investigators [23].

## 4. Conclusions

In this study, spectroscopic properties of studied compound have been theoretically determined through IR, NMR and UV–vis. Various quantum chemical calculations help us to identify the structural, conformational and spectral properties of studied molecule. In order to identify conformational structures, potential energy curve has been computed by means of scanning selected degree of essential torsional angles. Vibrational frequencies and $^{1}H$ and $^{13}C$ NMR chemical shifts of studied compound have been calculated

using density functional theory (B3LYP) method at 6-31G (*d*) basis set level. Detailed assignments with PED% analysis for selected vibrational frequencies have also been presented. Absorption wavelengths, excitation energies and assignments with major contributions of transitions are computed by TD-UHF method at 6-31G (*d*) basis set. We can say that calculated results of studied molecule are generally to be in a good agreement with experimental data. Besides, stability of tautomeric forms is investigated in present study. To find optimum transition states of studied molecule, QST2 approaches have been used by taking optimized azo-enol and hydrazo-keto form. Results of PES scans done by changing of bond length tautomeric O–H have shown that hydrazo-keto form of this molecule are more stable. Calculations of frontier molecular orbitals and first hyperpolarizability have confirmed this stability.

**Acknowledgments** This work is supported by Karamanoglu Mehmetbey University-Scientific Research Projects Coordinating Office (Grant No. 07-M-13).

## References

[1] J Koh and A J Greaves *Dyes Pigm.* **50** 117 (2001)
[2] H E Katz, K D Singer, J E Sohn, C W Dirk, L A King and H M Gordon *J. Am. Chem. Soc.* **109** 6561 (1987)
[3] T Abe, S Mano, Y Yamada and A Tomotake *J. Imaging Sci. Technol.* **43** 339 (1999)
[4] S Wang, S Shen and H Xu *Dyes Pigm.* **44** 195 (2000)
[5] K Maho et al. *Jpn. J. Appl. Phys.* **42** 1068 (2003)
[6] D W Rangnekar, V R Kanetkar, J V Malanker and G S Shankarling *Indian J. Fibre Text. Res.* **24** 142 (1999)
[7] G Hallas and J H Choi *Dyes Pig.* **40** 119 (1999)
[8] P Gregory, D R Waring and G Hallos *The Chemistry and Application of Dyes* (London: Plenum Press) p 18 (1990)
[9] S S Kandil *Transit. Metal Chem.* **23** 461 (1998)
[10] O E Woisetsclager, K Sünkel, W Weigand and W Beck *J. Organomet. Chem.* **584** 122 (1999)
[11] J W Daniel *Toxicol. Appl. Pharmacol.* **4** 572 (1962)
[12] M A Weaver and L Shuttleworth *Dyes Pigm.* **3** 81 (1982)
[13] H R Maradiya and V S Patel *Chem. Heterocycl. Compd.* **38** 1324 (2002)
[14] H S Bhatti and S Seshadri *Dyes Pigm.* **62** 83 (2004)
[15] [15] T H Afifi and A Z Sayed *J. Soc. Dyers Colour.* **113** 256 (2008)
[16] M A Metwally, E Abdel-Galil, A Metwally and F A Amer *Dyes Pigm.* **92** 902 (2012)
[17] A S Abd-El-Aziz and T H Afifi *Dyes Pigm.* **70** 8 (2006)
[18] G Hallas and A D Towns *Dyes Pigm.* **33** 215 (1997)
[19] G Hallas and A D Towns *Dyes Pigm.* **35** 45 (1997)
[20] F Karci and F Karci *Dyes Pigm.* **77** 451 (2008)
[21] F Karci, A Demirçalı, F Karci, I Kara and F Ucun *J. Mol. Struct.* **935** 19 (2009)
[22] F Ucun, A Saglam, I Kara and F Karci *J. Mol. Struct. Theochem.* **868** 94 (2008)
[23] F Karci and F Karci *J. Mol. Struct.* **1024** 117 (2012)
[24] S Gunasekaran and G R Ramkumaar *Indian J. Phys.* **83** 1549 (2009)
[25] D Mani, V T Bhat, K J Vinoy and E Arunan *Indian J. Phys.* **86** 225 (2012)
[26] G Mandal and T Ganguly *Indian J. Phys.* **85** 1229 (2011)
[27] M J Frisch et al. *GAUSSIAN 09, Revision D.01* (Pittsburgh: Gaussian Inc.) (2013)
[28] R Dennington II, T Keith and J Millam *GaussView Version 5.0* (Shawnee Mission: Semichem, Inc.) (2007)
[29] J B Foresman and A E Frisch *Exploring Chemistry with Electronic Structure Methods,*2nd edn (Pittsburgh: Gaussian, Inc.) (1996)
[30] M H Jamroz *Vibrational Energy Distribution Analysis VEDA 4* (Warsaw) (2004)
[31] M H Jamróz, J C Dobrowolski and R Brzozowski *J. Mol. Struct.* **787** 172 (2006)
[32] R Ditchfield **27** 786 (1974)
[33] C M Rohlfing, L C Allen R Ditchfield *Chem. Phys.* **87** 9 (1984)
[34] C Peng and H B Schlegel *Israel J. Chem.* **33** 449 (1993)
[35] C Peng, P Y Ayala, H B Schlegel and M J Frisch *J. Comp. Chem.* **17** 49 (1996)
[36] M Karakaya and F Ucun *Indian J. Phys.* **88** 119 (2014)
[37] M Karakaya and F Ucun *Russ. J. Phys. Chem.* A **88** 1147 (2014)
[38] M Karakaya and F Ucun *J. Struct. Chem.* **54** 321 (2013)
[39] N Subramanian, N Sundaraganesan and J Jayabharathi *Spectrochim. Acta Part A* **76** 259 (2010)
[40] Y Sun, X Chen, L Sun, X Guo and W Lu *Chem. Phys. Lett.* **381** 397 (2003)
[41] O Christiansen, J Gauss and J F Stanton *Chem. Phys. Lett.* **305** 147 (1999)
[42] R Zhang, B Du, G Sun and Y Sun *Spectrochim. Acta Part A* **75** 1115 (2010)
[43] S Muthu, G Ramachandran and J Uma maheswari *Spectrochim. Acta Part A* **93** 214 (2012)
[44] I Fleming *Frontier Orbitals and Organic Chemical Reactions* (London: Wiley) (1976)
[45] K Fukui *Science* **218** 747 (1982)
[46] P S Liyanage, R M de Silva and K M Nalin de Silva *J. Mol. Struct. Theochem.* **639** 195 (2003)
[47] I Guezguez et al. *Opt. Mater.* **36** 106 (2014)